

Cluster parameter determination and selection effects at a cluster sensitivity of $\sim 10^{-14}$ erg/s/cm² in [0.5-2 keV]

F. Pacaud, and the XMM-LSS consortium

Abstract: We discuss practical issues related to the construction of an X-ray cluster sample suitable for cosmological studies. The sensitivity for typical cluster sources is $\sim 10^{-14}$ erg/s/cm² in [0.5-2 keV]. The XMM PSF and background are assumed. Our results show that it is possible to gather an uncontaminated cluster sample using purely X-ray criteria, with a density of $\sim 6/\text{deg}^2$.

We demonstrate that, using a well adapted binning procedure, it is statistically possible to obtain a 20% temperature accuracy with only 200 photons for groups up to 2 keV. This subsequently enables us to show how selection effects – if ignored - can bias the determination of the evolution of the L-T relation. We also show that obtaining cluster masses (M_{500}) out to $z=1$ at the 30% level, with 10 ks XMM exposures, is not necessarily an unrealistic aim.

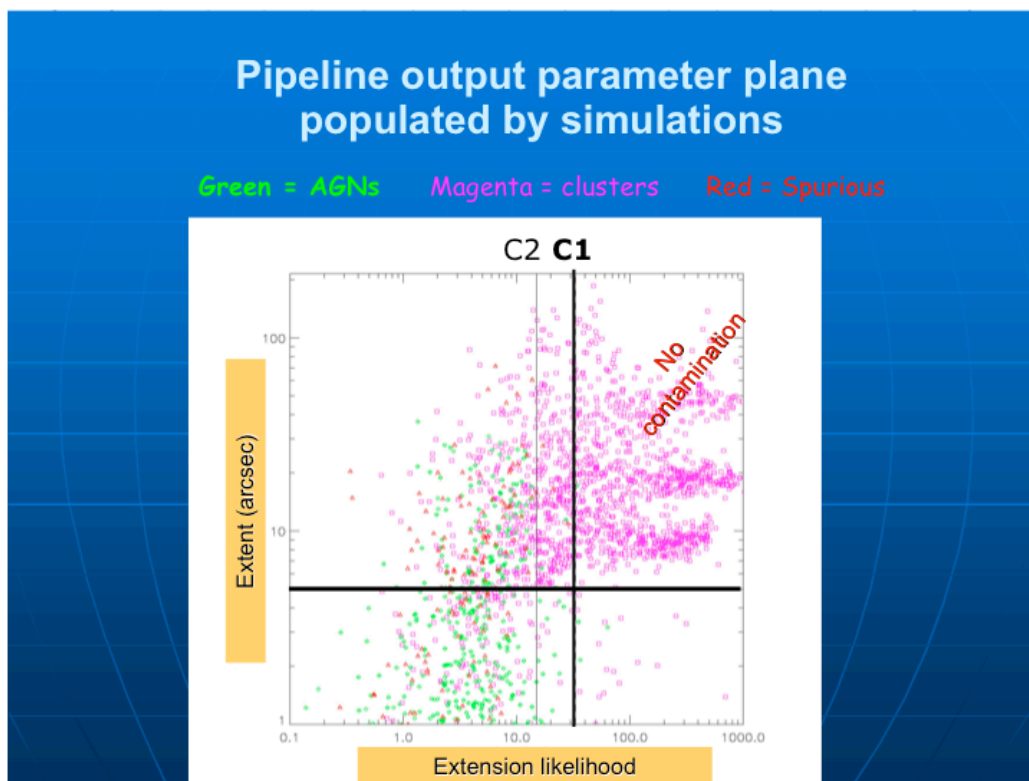


Fig.1 Selecting an uncontaminated cluster sample

The cosmological analysis of cluster samples requires the samples to be constructed from well-defined criteria. The selection parameters have, in turn, to be related with generic predictions from cosmological models of cluster evolution. It is thus essential to ensure that cleaning the sample from residual contamination (using e.g. optical confirmation) doesn't affect the overall selection effects.

One course of action is to obtain an uncontaminated cluster sample straight from the X-ray analysis. This is how we have defined the Class 1 sample, relying on simulated observations; it has a density of ~ 6 clusters/deg² for 10 ks XMM exposures. Relaxing the C1 criteria and allowing for $\sim 50\%$ contamination by point sources defines the C2 class (density of $\sim 12/\text{deg}^2$). cf PA06 for details.

Detection rates

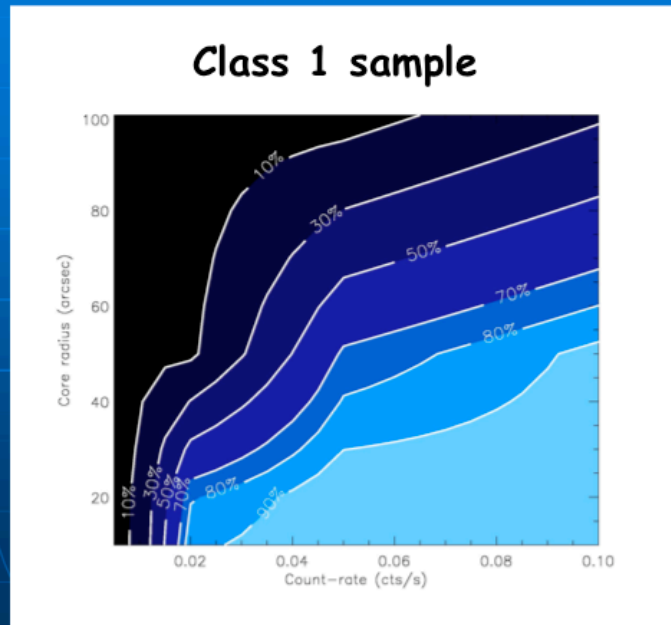


Fig2. Detection probabilities in a 2-D parameter space

The probabilities, for given selection criteria, are derived from the simulations performed in Fig. 1 and appear to depend both on the flux and the extent of the clusters almost regardless of the considered sample.

In particular, the largest uncontaminated sample with controlled selection effects is not flux limited, c.f. PA06.

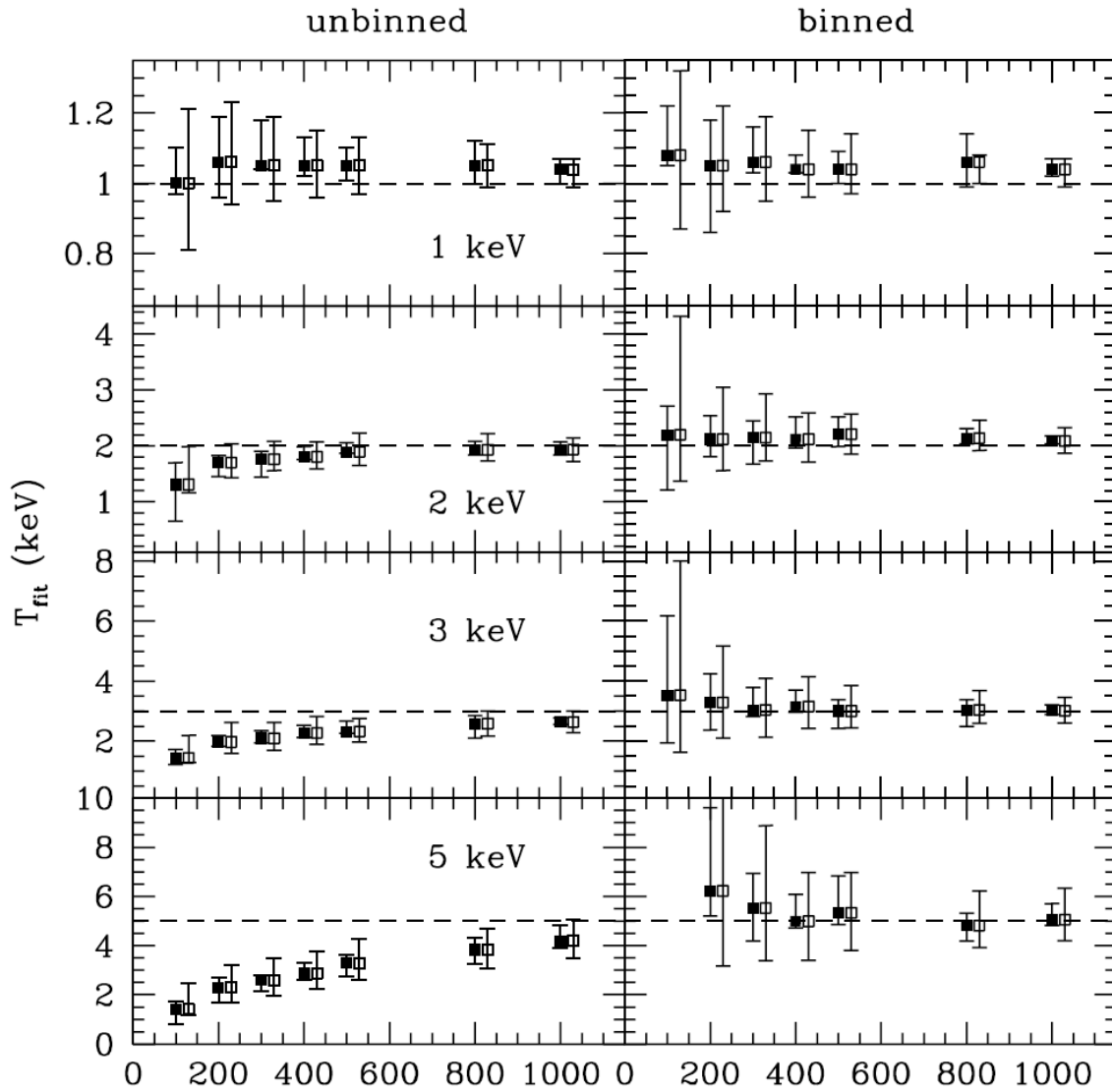


Fig3. Accuracy of cluster temperature measurements with 10 ks XMM exposures ($0.1 < z < 1$)

Using a well-adapted binning procedure, it is statistically possible to obtain a 20% temperature accuracy with only 200 photons for groups up to 2 keV. (W05)

The figure shows comparison of XSPEC computed temperatures for simulated group and cluster spectra employing the C-statistic with two different resampling approaches. Left-hand panels indicate the results for unbinned spectra. Right-hand panels indicate the results for binned spectra such that the background spectrum displays a minimum of five counts per spectral bin. Panels in each row correspond to spectral models with the indicated input temperature (also shown by the horizontal dashed line). In each panel, data points represent the mean XSPEC computed temperature returned from the set of simulated spectra as a function of total input counts. Filled squares plus error bars indicate the mean computed temperature and the distribution of temperatures accounting for 68 per cent of the sample. Open squares plus error bars indicate the mean computed temperature and the median 1σ uncertainty returned by XSPEC (open squares are shifted to the right by 30 counts with respect to the filled squares for clarity).

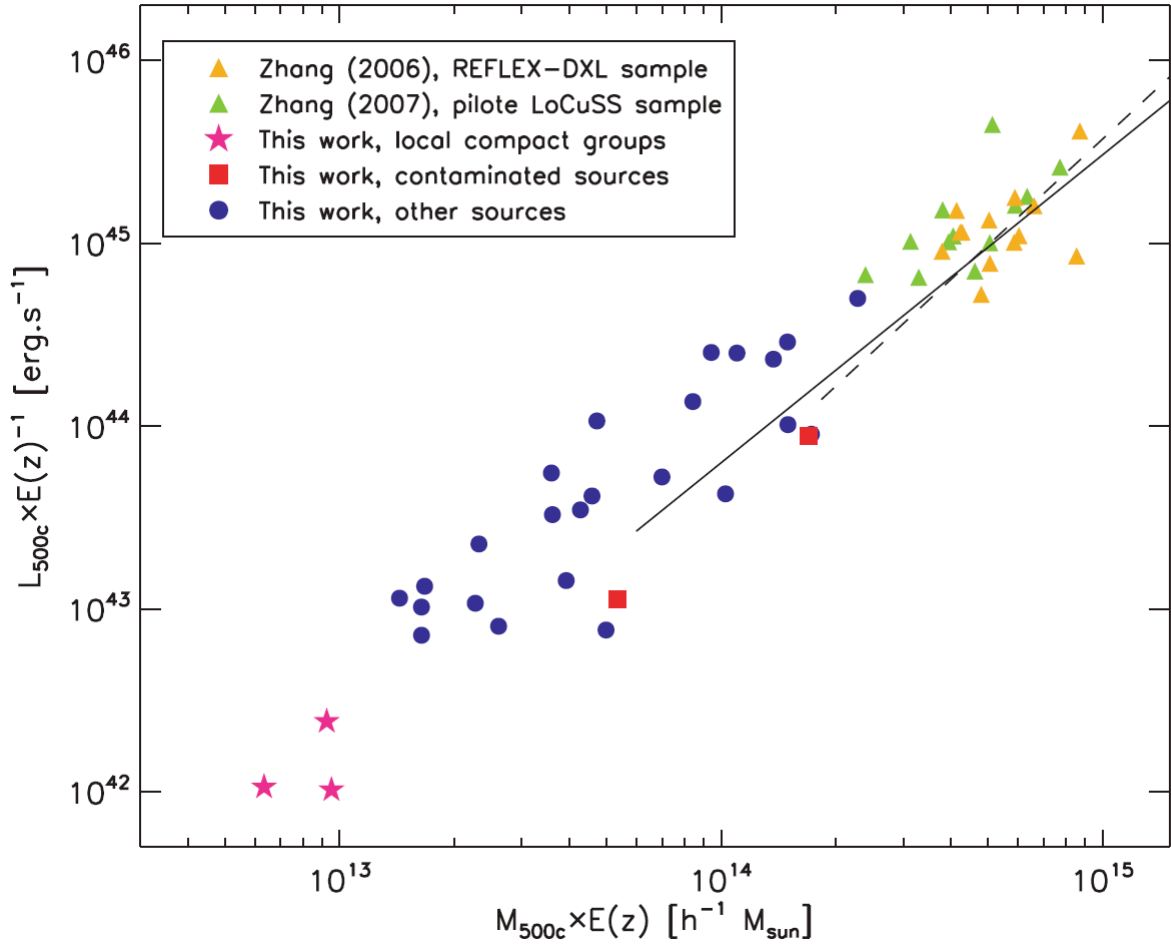


Fig. 4 Cluster mass measurements with 10 ks XMM exposure ($0.1 < z < 1$)

The cluster masses were determined assuming isothermality + hydrostatical equilibrium and a density profile derived by the surface brightness profile.

The mass–luminosity relation for 29 C1 clusters. Because of the large redshift range spanned by the data, the mass and luminosity parameters are scaled assuming self-similar evolution [factor $E(z)$]. For comparison, the massive cluster samples from Zhang et al. (2006) and Zhang et al. (2007) are also shown. The dashed and solid lines also show the mean M500–LX relation inferred from the M500–T and LX–T measured in Arnaud et al. (2005) and Arnaud & Evrard (1999), respectively, for $T > 3.5$ keV and $T > 2$ keV. It is important to keep in mind, that given the variety of cluster histories and dynamical state, there is a large intrinsic dispersion in the L–M relation (cf PA07).

Note on the mass accuracy:

The mass of XLSS 29 at $z = 1.05$ (second most luminous blue point) was measured to be $1.4 \cdot 10^{14} M_{\odot}$ with survey data (total photon number = 355; P07) and $1.8 \pm 0.5 \cdot 10^{14} M_{\odot}$ from a subsequent 80 ks XMM pointing (Maughan et al 2007).

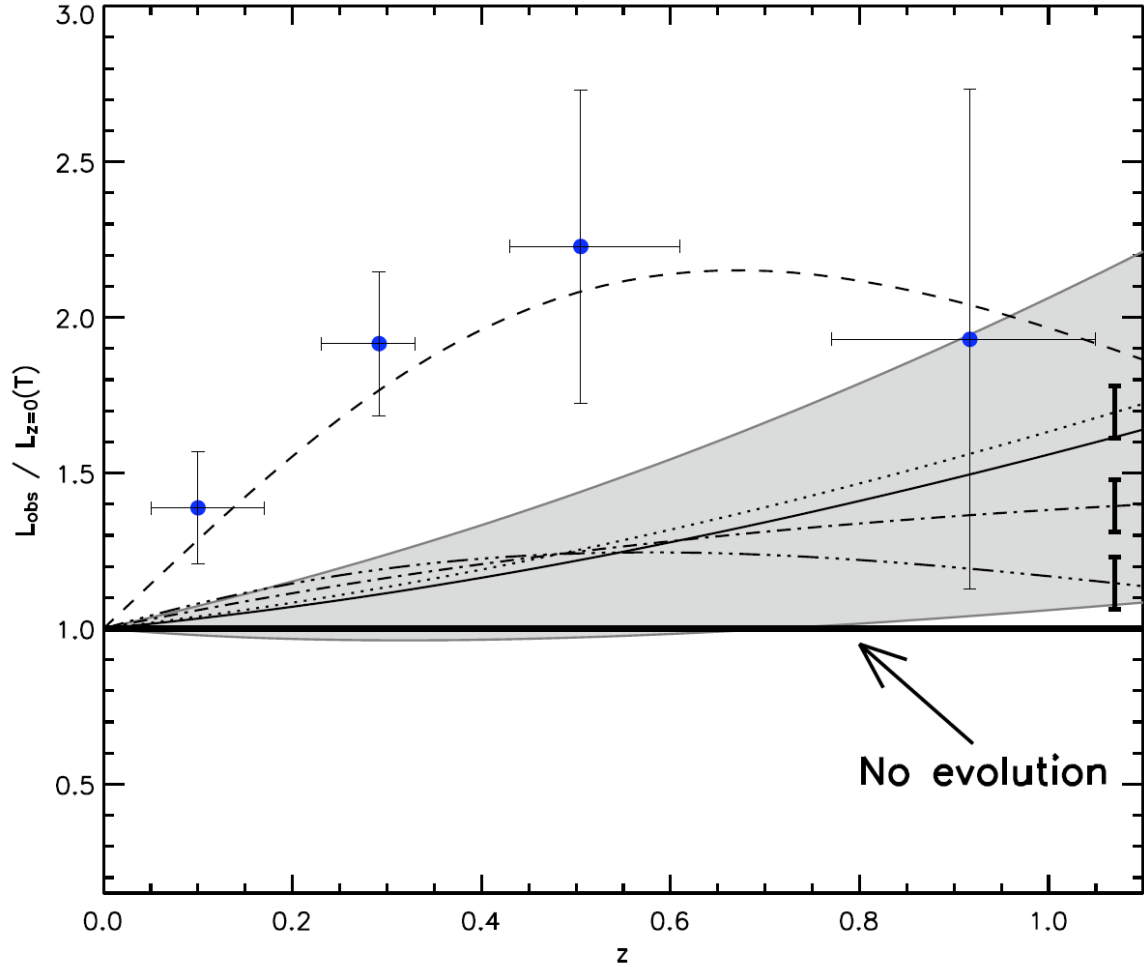


Fig. 5 Constraining the evolution of the L-T relation from 10ks survey data.

Impact of the sample selection function.

The graph shows the cluster X-ray luminosity enhancement with respect to the expectation at $z = 0$. The 29 C1 clusters are sorted in 4 redshift intervals. The dash line is the result of an ad hoc two-parameter fit to the raw data points: $(1+z)^\alpha \times E(z)^\beta$ with $\alpha = 4.7$, $\beta = -5.4$. When the survey selection function is taken into account, the best fit is the solid line, $(1+z)^\alpha E(z)$ with $\alpha = -0.07$, which is very close to the evolution predicted by the self-similar model (dotted line, $\alpha = 0$). The grey region delineates the 1σ confidence interval for the surveyed 5 deg². The dot-dash and triple-dot-dash lines are the evolutionary models by Voit (2005) including non-gravitational physics. The thick error bars at the end of the three models indicate the 1σ range expected for a 200 deg² survey.

The fact that selection effects were not systematically considered in the former L-T(z) studies may explain the discordant results obtained so far: because the cluster mass function is so steep, most clusters are detected around the survey limiting sensitivity, hence favouring the compilation of over-luminous objects at any redshift. This feature is certainly not unique to the XMM-LSS survey, but rather of any X-ray cluster survey (provided that the detection is performed down to the capabilities of the survey). This bias is to affect any sub-sample “randomly” selected from all sky or serendipitous surveys for subsequent deep XMM or Chandra temperature observations (cf PA07).

Further, we have shown that, in order to increase the precision of the L-T relation evolution, it is more efficient to increase the cluster sample than the accuracy on the temperature measurements (see second contribution by Pacaud).

References:

Maughan, B., et al: 2007, MNRAS submitted (astro-ph/07092300)

Pacaud, F. et al (PA06): 2006, MNRAS 372, 578

Pacaud, F et al (PA07): 2007, MNRAS 382, 1289

Voit, M.: 2005, Rev. Mod. Phys 77, 207

Willis, J., et al (W05): 2005, MNRAS 363, 675